Biomedicine & Pharmacotherapy 167 (2023) 115436

Contents lists available at ScienceDirect

Biomedicine & Pharmacotherapy

journal homepage: www.elsevier.com/locate/biopha

Antitumor activity of alkylphospholipid edelfosine in prostate cancer models and endoplasmic reticulum targeting

EL-Habib Dakir [a,b,*,1], Consuelo Gajate [a,c,2], Faustino Mollinedo [a,c,**,3]

[a] Instituto de Biología Molecular y Celular del Cáncer, Centro de Investigación del Cáncer, CSIC-Universidad de Salamanca, Campus Miguel de Unamuno, E-37007 Salamanca, Spain
[b] Faculty of Biology, University of Latvia, Riga, Latvia
[c] Laboratory of Cell Death and Cancer Therapy, Department of Molecular Biomedicine, Centro de Investigaciones Biológicas – Margarita Salas, Consejo Superior de Investigaciones Científicas (CSIC), Ramiro de Maeztu 9, E-28040 Madrid, Spain

ARTICLE INFO

Keywords:
Edelfosine
Alkylphospholipid analog
MPAKT transgenic animal model
Xenograft animal model
Endoplasmic reticulum
Prostate cancer

ABSTRACT

Prostate cancer is the second most frequent cancer and the fifth leading cause of cancer death among men worldwide. While the five-year survival in local and regional prostate cancer is higher than 99%, it falls to about 28% in advanced metastatic prostate cancer. The ether lipid edelfosine is considered the prototype of a family of promising antitumor drugs collectively named as alkylphospholipid analogs. Here, we found that edelfosine was the most potent alkylphospholipid analog in inducing apoptosis in three different human prostate cancer cell lines (LNCaP, PC3, and DU145) with distinct androgen dependency, and differing in tumor suppressor phosphatase and tensin homolog (PTEN) and p53 status. Edelfosine accumulated in the endoplasmic reticulum of prostate cancer cells, leading to endoplasmic reticulum stress and cell death in the three prostate cancer cells. Inhibition of autophagy potentiated the pro-apoptotic activity of edelfosine in LNCaP and PC3 cells, where autophagy was induced as a survival response. Edelfosine induced a slight and transient inhibition of AKT in PTEN-negative LNCaP and PC3 cells, but not in PTEN-positive DU145 cells. Daily oral administration of edelfosine in murine prostate restricted AKT kinase transgenic mice, expressing active AKT in a prostate-specific manner, and in a DU145 xenograft mouse model resulted in significant tumor regression and apoptosis in tumor cells. Taken together, these results show a significant *in vitro* and *in vivo* antitumor activity of edelfosine against prostate cancer, and highlight the endoplasmic reticulum as a novel and promising therapeutic target in prostate cancer.

1. Introduction

Prostate cancer is the second most frequently occurring cancer in men after lung cancer, and it was the fifth leading cause of cancer death among men worldwide in 2020 [1]. Prognosis of prostate cancer patients is highly dependent on clinical stage (localized, locally advanced or advanced), Gleason score and prostate-specific antigen (PSA) level [2,3]. While the five-year survival in local and regional prostate cancer is

Abbreviations: APLs, alkylphospholipid analogs; ATF3, activating transcription factor 3; BODIPY, boron-dipyrromethene; ER, endoplasmic reticulum; ET-18-OCH_3, (1-*O*-octadecyl-2-*O*-methoxy-*rac*-glycero-3-phosphocholine); Et-BDP-ET, 1-*O*-[11′-(6′′-ethyl-1′′,3′′,5′′,7′′-tetramethyl-4′′,4′′-difluoro-4′′-bora-3a′′,4a′′-diaza-*s*-indacen-2′′-yl)undecyl]– 2-*O*-methyl-*rac*-glycero-3-phosphocholine; H&E, hematoxylin and eosin; LC3, microtubule-associated protein 1 light chain 3; MPAKT mice, murine prostate restricted AKT kinase transgenic mice; PBS, phosphate-buffered saline; PIN, prostate intraepithelial neoplasia; PTEN, phosphatase and tensin homolog; RFP, red fluorescent protein; SCID, severe combined immunodeficiency; VP, ventral prostate.

* Corresponding author at: Instituto de Biología Molecular y Celular del Cáncer, Centro de Investigación del Cáncer, CSIC-Universidad de Salamanca, Campus Miguel de Unamuno, E-37007 Salamanca, Spain.
** Corresponding author at: Laboratory of Cell Death and Cancer Therapy, Department of Molecular Biomedicine, Centro de Investigaciones Biológicas – Margarita Salas, Consejo Superior de Investigaciones Científicas (CSIC), Ramiro de Maeztu 9, E-28040 Madrid, Spain.
E-mail addresses: dakir@usal.es (E.-H. Dakir), consuelogajate@gmail.com (C. Gajate), fmollin@cib.csic.es (F. Mollinedo).
[1] https://orcid.org/0000-0002-8482-3412
[2] https://orcid.org/0000-0003-0604-6459
[3] https://orcid.org/0000-0002-4939-2434

https://doi.org/10.1016/j.biopha.2023.115436
Received 13 June 2023; Received in revised form 31 August 2023; Accepted 31 August 2023
Available online 8 September 2023

approaching 100%, it falls to about 28% in advanced metastatic prostate cancer [4]. About 90% of men with advanced prostate cancer develop bone metastases [5]. The 5-year survival drops to a dismal 3% for patients with bone metastases at initial diagnosis [6]. Advanced metastatic prostate cancer remains incurable, thus highlighting the need for more effective treatments at this stage of the disease. Treatment options include surgery, hormonal therapy, chemotherapy, immunotherapy, radiation, as well as a combination of the above [7–9]. However, despite most metastatic prostate cancer respond initially to androgen deprivation, almost all patients will eventually progress to metastatic castration-resistant prostate cancer (mCRPC), a term that refers to a cancer that has metastasized beyond the prostate gland, and for which hormone therapy is no longer effective. Some drugs used to treat metastatic prostate cancer, improving overall survival, include: docetaxel, usually combined with prednisone, cabazitaxel, mitoxantrone, estramustine, abiraterone, enzalutamide, apalutamide, and Lutetium-177 (^{177}Lu)–PSMA-617 [10–12]. Nevertheless, despite a good initial response and survival benefit, nearly all patients eventually develop drug resistance, which is a key stumbling block to long-term survival. In addition, most current treatments have adverse effects that can negatively affect quality of life [7,13]. Thus, new therapeutic approaches and chemotherapeutic agents with no or few side effects are needed.

The so-called alkylphospholipid analogs (APLs) constitute a heterogeneous family of unnatural lipids that target cell membranes and promote apoptosis in a wide variety of tumor cells [14–17]. Among these APLs, edelfosine [ET-18-OCH_3, (1-*O*-octadecyl-2-*O*-methoxy-*rac*-glycero-3-phosphocholine)], considered the APL prototype compound, stands out as for its ability to induce apoptosis in a wide variety of malignant cells in a rather selective way [18,19], through lipid raft reorganization in hematological cancer cells [20–29] and through its accumulation in the endoplasmic reticulum (ER) in solid tumor cells [26,30–33], with no significant side effects or low toxicity profile [34]. In addition, oral administration of edelfosine induces a potent antitumor activity in different xenograft animal models for a number of tumors, including pancreatic cancer [31], Ewing's sarcoma [32], multiple myeloma [24], mantle cell lymphoma [25], and chronic lymphocytic leukemia [25].

Prostate cancer cells are highly secretory, and the ER is the organelle involved in the synthesis and maturation of proteins that are heading for the secretory pathways [35]. Furthermore, ultrastructural analysis of prostate tumor tissue shows prominent and numerous vesicles of granular ER [36]. Here, we present evidence, by using different *in vitro* and *in vivo* prostate cancer models, that edelfosine exerts a significant antitumor activity against prostate cancer, promoting apoptosis by targeting the ER.

2. Materials and methods

2.1. Drugs and reagents

Edelfosine was obtained from R. Berchtold (Biochemisches Labor, Bern, Switzerland). Edelfosine stock solutions were prepared as previously described [18]. Briefly, edelfosine was dissolved at 2 mM, as a stock solution, by heating at 50 °C for 45 min in RPMI-1640 culture medium (Invitrogen, Carlsbad, CA, USA), containing 10% (v/v) heat-inactivated fetal bovine serum (Gibco Life Technologies, Waltham, MA, USA). The clear solution was sterilized by filtration through a 0.22 μm pore size Millipore sterile filter (Millipore Corporation, Burlington, MA, USA) and stored at 4 °C until use. Miltefosine (hexadecylphosphocholine) and perifosine (octadecyl-(1,1-dimethyl-piperidinio-4-yl)-phosphate) were from Shelleckchem (Houston, TX, USA). Erucylphosphocholine [(13*Z*)-docos-13-en-1-yl 2-(trimethylammonio) ethyl phosphate] was kindly provided by Zentaris (Frankfurt, Germany). Erufosine (erucylphosphohomocholine) was kindly provided by Dr. Lars Lindner (Ludwig-Maximilians-University, Munich, Germany). Stock sterile solutions of the distinct APLs (2 mM) were prepared in RPMI-1640 culture medium, supplemented with 10% (v/v) heat-inactivated fetal bovine serum, as above. The pan-caspase inhibitor carbobenzoxy-valyl-alanyl-aspartyl-[*O*-methyl]-fluoromethylketone (z-VAD-fmk) was from Alexis Biochemicals (San Diego, CA, USA). Bafilomycin A1 was from Sigma-Aldrich (St. Louis, MO, USA). Acrylamide/Bisacrylamide, ammonium persulfate, and N,N,N′,N′-tetramethylethylenediamine were from Bio-Rad (Hercules, CA, USA). Immobilon-P polyvinylidene difluoride (PVDF) membranes, Hybond ECL nitrocellulose membranes and ECL Western Blotting Detection Reagents were from GE Healthcare (Chicago, IL, USA). DAPI was from Molecular Probes (Carlsbad, CA, USA).

2.2. Cell culture

Human prostate cancer cell lines LNCaP (p53 wild-type, phosphatase and tensin homolog [PTEN]-negative, androgen-sensitive, highly differentiated), PC3 (p53$^{-/-}$, PTEN-negative, androgen-independent, poorly differentiated), and DU145 (p53 mutant, PTEN-positive, androgen-independent, moderately differentiated) were obtained from American Type Culture Collection (ATCC) (Manassas, VA, USA), and grown in RPMI-1640 medium (Invitrogen), supplemented with 10% (v/v) heat-inactivated fetal bovine serum, 100 U/ml penicillin, 100 μg/ml streptomycin and 2 mM L-glutamine (Gibco Life Technologies) at 37 °C in a humidified atmosphere containing 5% CO_2. All cell lines were tested for mycoplasma contamination using MycoProbe Mycoplasma Detection Kit (R&D systems, Abingdon, UK). Exponentially growing cells were treated with the corresponding APLs at the indicated concentrations and incubation times. Samples were analyzed by flow cytometry to determine apoptosis through cell cycle analyses.

2.3. Apoptosis assay

Quantification of apoptotic cells was determined by flow cytometry as the percentage of cells at the sub-G_0/G_1 region (hypodiploidy) in cell cycle analysis, as previously described [37]. Briefly, after each treatment, cells were centrifuged and fixed overnight in ethanol 70% (v/v) at 4 ºC. Then, cells were pelleted by centrifugation (288 x *g*, 7 min) and incubated for 1 h at room temperature, in the dark, with 0.2 mg/ml RNase A and 10 μg/ml propidium iodide. The percentages of cells in each cycle phase were determined using a FC500-MPL (Beckman-Coulter, Brea, CA, USA) flow cytometer. Cell cycle profiles were generated using manually drawn gates with Cyflogic software (Perttu Terho, Mika Korkeamaki, CyFlo Ltd, Turku, Finland), and the percentage of cells in the sub-G_0/G_1 region (apoptotic cells with hypodiploid DNA content) was quantified as previously described [37].

2.4. Confocal microscopy

The subcellular localization of edelfosine in prostate cancer cells was analyzed using the edelfosine analog 1-*O*-[11′-(6′′-ethyl-1′′,3′′,5′′,7′′-tetramethyl-4′′,4′′-difluoro-4′′-bora-3a′′,4a′′-diaza-*s*-indacen-2′′-yl) undecyl]−2-*O*-methyl-*rac*-glycero-3-phosphocholine (Et-BDP-ET) [38,39], containing a boron-dipyrromethene (BODIPY) molecule, a kind gift from Dr. F. Amat-Guerri and Dr. A.U. Acuña (Consejo Superior de Investigaciones Científicas, Madrid, Spain). ER was visualized by using the CellLight™ ER-red fluorescent protein (RFP) BacMam 2.0 reagent (ThermoFisher, Waltham, MA, USA), following the manufacturer's specifications as previously described [39]. This CellLight™ ER-RFP BacMam 2.0 reagent includes a fusion construct of TagRFP with the ER signal sequence of calreticulin and KDEL (ER retention signal), providing accurate and specific targeting to cellular ER with minimal cellular disruption. Cells were then incubated for 3 h with 20 μM Et-BDP-ET as previously described [39]. Colocalization of both signals (RFP; Excitation: 555 nm, Emission: 574–627 nm; BODIPY: Excitation: 498 nm, Emission: 510–549 nm) was analyzed by excitation of both fluorochromes in the same section. Fluorescence was visualized with a

confocal laser scanning microscope Leica TCS SP8 STED 3X (Wetzlar, Germany), fitted with a 405 nm UV laser and a white-light laser with freely tunable excitation (470–670 nm).

To detect nuclear translocation of activated caspase-3 to the nucleus, cells were attached to sterile poly-L-lysine-coated round glass micro coverslips, and then fixed with 2% or 4% formaldehyde in phosphate-buffered saline (PBS) as previously described [40]. Following cell permeabilization with 0.1% Tween-20 for 5 min, and washing twice with PBS, cells were incubated with anti-cleaved caspase-3 rabbit monoclonal antibody (Abcam, Cambridge, UK) (1:100 dilution in PBS) overnight in a humid atmosphere at 4 °C. Then, slides were washed twice with PBS, and incubated with a Cy3-conjugated anti-rabbit IgG antibody (Abcam) (diluted 1:100 in PBS). DAPI was used at dilution of 1:1000 in PBS for nuclear staining. Images were taken with a Zeiss confocal laser scanning microscope (Oberkochen, Germany) at 67x magnification.

2.5. Western blot analysis

Cells were harvested in a lysis buffer (25 mM HEPES, pH 7.7, 0.3 M NaCl, 1.5 mM $MgCl_2$, 0.2 mM EDTA, 0.1% Triton X-100, 20 mM β-glycerophosphate, 0.1 mM Na_3VO_4), supplemented with protease inhibitors (1 mM phenylmethylsulfonyl fluoride, 20 μg/ml aprotinin, 20 μg/ml leupeptin) or a protease inhibitor cocktail (Roche, Basel, Switzerland), and protein concentration was determined using a Bradford assay (ThermoFisher, Waltham, MA, USA). Proteins (30–40 μg/lane) were run in SDS polyacrylamide gels, transferred to Immobilon-P PVDF or nitrocellulose membranes, blocked with 5% (w/v) non-fat dry milk in 50 mM Tris-HCl (pH 8.0), 150 mM NaCl, 0.1% Tween 20 (TBST) with gentle shaking for 60–90 min at room temperature, and incubated for 1 h at room temperature or overnight at 4 ºC with the following specific antibodies: anti-poly(ADP-ribose) polymerase mouse monoclonal antibody (1:1000, BD Pharmingen); anti-CHOP/GADD153 rabbit monoclonal antibody (1:250, Santa Cruz Biotechnology); anti-p-ERK1/2 rabbit polyclonal antibody (1:1000, Cell Signaling Technology); anti-ERK2 mouse monoclonal antibody (1:1000, Santa Cruz Biotechnology); anti-LC3 (microtubule-associated protein 1 light chain 3) rabbit polyclonal antibody (1:1000, Cell Signaling Technology); anti-Ser473 p-AKT rabbit polyclonal antibody (1:3000, Cell Signaling); anti-AKT1/2/3 rabbit polyclonal antibody (1:1000, Santa Cruz Biotechnology); and anti-β-actin mouse monoclonal antibody (1:5000, Sigma). After three 5-min TBST washes, the membranes were incubated with horseradish peroxidase (HRP)-conjugated secondary anti-rabbit or anti-mouse antibodies (1:1000 dilution, Abcam) for 1 h at room temperature. Then, the protein bands were visualized with a ChemiDoc™ Imaging System (Bio-Rad), using an enhanced chemiluminescence detection kit (GE Healthcare).

2.6. MPAKT transgenic animal model and genotyping

Murine prostate restricted AKT kinase activity was generated in transgenic mice (MPAKT mice) [41], using probasin prostate-specific tissue promoter and Myr-HA tag epitope. A cDNA directing the expression of myr and HA epitope-tagged human *Akt-1* was inserted 3′ of the rat probasin promoter -426 to +28 bp (rPb-myr-HA-AKT1 transgene), as described [41,42]. The MPAKT transgenic model expresses active AKT in the prostate and has been previously used to study the role of AKT in prostate epithelial cell transformation and in the discovery of molecular markers relevant to human disease and drug targets [43,44]. Genotyping of the resultant pups was done by extracting tail DNA using Red-Extract (Sigma–Aldrich) as described [45], and two specific sets of primers for PCR as previously reported [46]. DNA was visualized after electrophoresis by ethidium bromide staining. Transgenic MPAKT mice carrying *Akt* gene and wild-type mice were randomly assigned to cohorts of 10 mice each, receiving a daily oral administration of edelfosine (30 mg/kg of body weight), a drug dose and schedule previously used in *in vivo* studies with no significant toxicity [24,25,31,32], or an equal volume of vehicle (water). The animals were euthanized 24 h after the last drug administration according to institutional guidelines, and following procedures approved by the Ethics Committee of the University of Salamanca, complying with the European Union (European Directive 2010/63/EU) guidelines for animal experiments. A necropsy analysis involving prostate organ and distinct organs was carried out.

2.7. Xenograft animal model

All animal experiments were approved by the Ethics Committee of the University of Salamanca (Salamanca, Spain). All mouse experimental procedures were performed according to the protocols approved by and conducted at the accredited Animal Experimentation Facility of the University of Salamanca (register No. PAE/SA/001), and complied with the Spanish (RD1201/05) and the European Union (European Directive 2010/63/EU) guidelines on animal experimentation for the protection and humane use of laboratory animals. Male CB17-severe combined immunodeficiency (SCID) mice (8 weeks old) (Charles River Laboratories, Wilmington, MA, USA), kept and handled according to institutional guidelines, complying with Spanish legislation under 12/12 h light/dark cycle at a temperature of 22 °C, received a standard diet and acidified water *ad libitum*. DU145 cells (5×10^6) were injected subcutaneously in 100 μl PBS together with 100 μl Matrigel basement membrane matrix (Becton Dickinson) into the right flank of each mouse. When tumors were palpable, approximately two weeks after tumor cell implantation, mice were randomly assigned to cohorts of 10 mice each, receiving a daily oral administration of edelfosine (30 mg/kg of body weight), a drug dose and schedule previously used with no significant toxicity in different CB17-SCID mice [24,25,31,32], or an equal volume of vehicle (water), for 8 weeks. Volume determination of subcutaneous xenograft tumors *in vivo* was by the use of external calipers to measure the shortest and longest diameters of the tumors at the indicated time intervals. Tumor volume (mm^3) was calculated using the following standard ellipsoid formula: (the shortest diameter)^2 × (the longest diameter) × 0.5 [24,25,31,32,47,48]. Animal body weight and any sign of morbidity were monitored. Drug treatment lasted 8 weeks. Animals were euthanized 24 h after the last drug administration according to institutional guidelines, and then tumors were carefully removed, measured, weighed and analyzed. A necropsy analysis involving tumors and distinct organs was carried out.

2.8. Histochemical analysis

Tumor tissue samples were fixed in 4% (w/v) phosphate-buffered paraformaldehyde and embedded in paraffin. Wax tissue sections (4–5 μm) were deparaffinized and hydrated in graded ethanol and distilled water. Endogenous peroxidase activity was blocked using methanol and 3% H_2O_2 for 30 min as previously described [45]. Histological sections were counterstained with hematoxylin and eosin (H&E). Sections were subsequently counterstained with Mayer's hematoxylin or Light Green. Staining was analyzed with a Nikon Eclipse 400® microscope and Metamorph® software (Molecular Devices Corporation, San Jose, CA). Apoptotic cells were identified by well-established morphological criteria on H&E-stained slides, including [49,50]: nuclear pyknosis (due to chromatin condensation), nuclear karyorrhexis (nuclear fragmentation), hypereosinophilic cytoplasm (due to cytoplasmic condensation), cell shrinkage. The number of apoptotic cells was determined blindly by two observers, and is reported as the percentage of cells undergoing apoptosis per high-powered field.

2.9. Statistical analysis

Results are shown as means ± SD of the number of experiments indicated. Statistical evaluation was performed by Student's *t*-test to estimate the true difference between two group means, and by ANOVA to compare more than two groups. A *P*-value of < 0.05 was considered

statistically significant.

3. Results

3.1. Edelfosine inhibits tumor development in the transgenic MPAKT mouse prostate model

The MPAKT model, which expresses constitutively activated AKT in mouse prostate epithelial cells, promotes prostate intraepithelial neoplasia (PIN) by prostate restricted AKT activation [41], and recapitulates a number of elements and phenotypes common to prostate cancer observed in humans, being a useful model to generate prostate epithelial cell transformation [41]. Thus, we reproduced the MPAKT model, and Supplementary Figure S1 shows the major features of this MPAKT murine model as compared to wild-type mice. Unlike wild-type mice, transgenic MPKAT mice carried the *Akt* transgene and showed bladder obstruction and an increased prostatic epithelial hyperplasia (Supplementary Figure S1). We used the MPAKT transgenic model as a murine model to analyze the antitumor effect of orally administered edelfosine against prostate cancer. Three cohorts ($n = 10$ mice in each group) of untreated wild-type mice (water vehicle), untreated transgenic MPAKT mice (water vehicle), and edelfosine-treated MPAKT mice were analyzed to determine the *in vivo* antitumor activity of edelfosine against prostate cancer (Fig. 1A). Interestingly, daily oral administration of MPAKT transgenic mice with edelfosine (30 mg edelfosine/kg of body weight) or placebo (water) (Fig. 1A) for 8 weeks led to a drastic inhibition of the bladder obstruction and tumor regression (Fig. 1B). Histological studies of the ventral prostate (VP) from the MPAKT mice revealed a striking phenotype characterized by a hyperplastic and dysplastic epithelium with disorganized multicell layers, intraepithelial lumen formation, loss of cell polarity and nuclear atypia (Fig. 1C), which were consistent with PIN. However, H&E staining in paraffin embedded sections of VP tissue from edelfosine-treated MPAKT transgenic showed a dramatic PIN inhibition and tissue patterns that resembled those of untreated wild-type mice (Fig. 1C). Furthermore, tissue sections, stained with H&E, showed irregular cells with hypereosinophilic cytoplasm and nuclear karyorrhexis and/or pyknosis, characteristic of cell death by apoptosis (Fig. 1C) in edelfosine-treated mice. These results suggest that oral treatment of edelfosine induced a decrease in prostatic epithelial hyperplasia that could be in part due to the induction of apoptosis.

3.2. Edelfosine induces apoptosis in different human prostate cancer cells through its accumulation in the ER and subsequent ER stress

Next, we analyzed the pro-apoptotic activity of edelfosine and several additional clinically relevant APLs (miltefosine, perifosine and erucylphosphocholine) [16,19,51–55], at 10 and 20 μM, on three different established human prostate cancer cell lines, namely: LNCaP, PC3 and DU145, used as standard prostate cancer cell lines in therapeutic research [56,57]. LNCaP (Lymph Node Carcinoma of the Prostate) is an androgen-sensitive, PTEN-negative, human prostate adenocarcinoma cell line derived from a lymph node metastasis [58,59]; DU145 is an androgen-independent, PTEN-positive, human prostate adenocarcinoma cell line derived from a central nervous system metastasis [60]; and PC3 is an androgen-independent, PTEN-positive, human prostate adenocarcinoma cell line derived from bone metastasis [61,62]. Time course and dose-response experiments showed that edelfosine induced first a G_2/M arrest, before the onset of apoptosis (Fig. 2A). Edelfosine was the most effective APL in inducing apoptosis in the three prostate cancer cell lines, with LNCaP cells being the most sensitive ones (Fig. 2B). The apoptosis response is both dose- and time-dependent (Fig. 2B). APLs ranked edelfosine

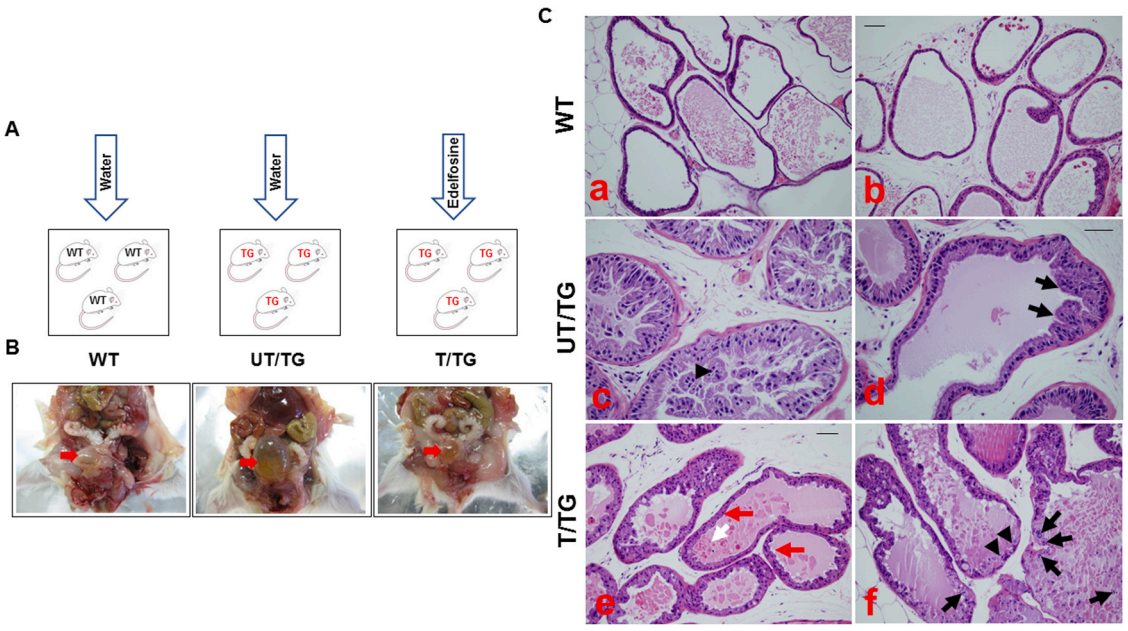

Fig. 1. *In vivo* antitumor activity of edelfosine in MPAKT transgenic mice. A. Oral administration of either water (untreated, UT) or edelfosine (30 mg/kg) (treated, T) to mice distributed in three groups ($n = 10$ in each cohort) as untreated wild-type (WT), untreated MPAKT transgenic mice (UT/TG) and edelfosine-treated MPAKT transgenic mice (T/TG). **B.** Mice necropsy showing prostate organ and ureter in representative mice. Orally administered edelfosine reduced bladder and ureteral obstruction in MPAKT transgenic mice (red arrow). Data shown in this figure are representative of 10 mice analyzed in each cohort. **C.** Ventral prostate (VP) tissue was harvested during necropsy and organ collection, paraffin embedded, and 5 μm sections were stained for H&E. Regions of the prostate anatomy were assessed by light microscopic examination with H&E staining in WT and MPAKT transgenic (TG) mice, untreated (UT) and treated (T) with edelfosine. WT mice show normal prostate organs (Cab) (x200 magnification; scale bar, 50 μm). AKT activation induces PIN and dysplasia in untreated MPAKT transgenic mice (UT/TG). Features of PIN include loss of cell polarity and dysplasia (black head arrow in Cc, and black arrows in Cd) (x400 magnification; scale bar, 50 μm). Edelfosine-treated MPAKT mice (T/TG) show tumor regression and cell death induction (Cef) (x200 magnification; scale bar, 50 μm). PIN regression was observed in transgenic mice treated with edelfosine (red arrow, Ce), as well as cell death and loss of DNA (white arrow, Ce), nuclear atypia (black head arrow, Cf), and nuclear karyorrhexis and/or pyknosis (black arrow, Cf).

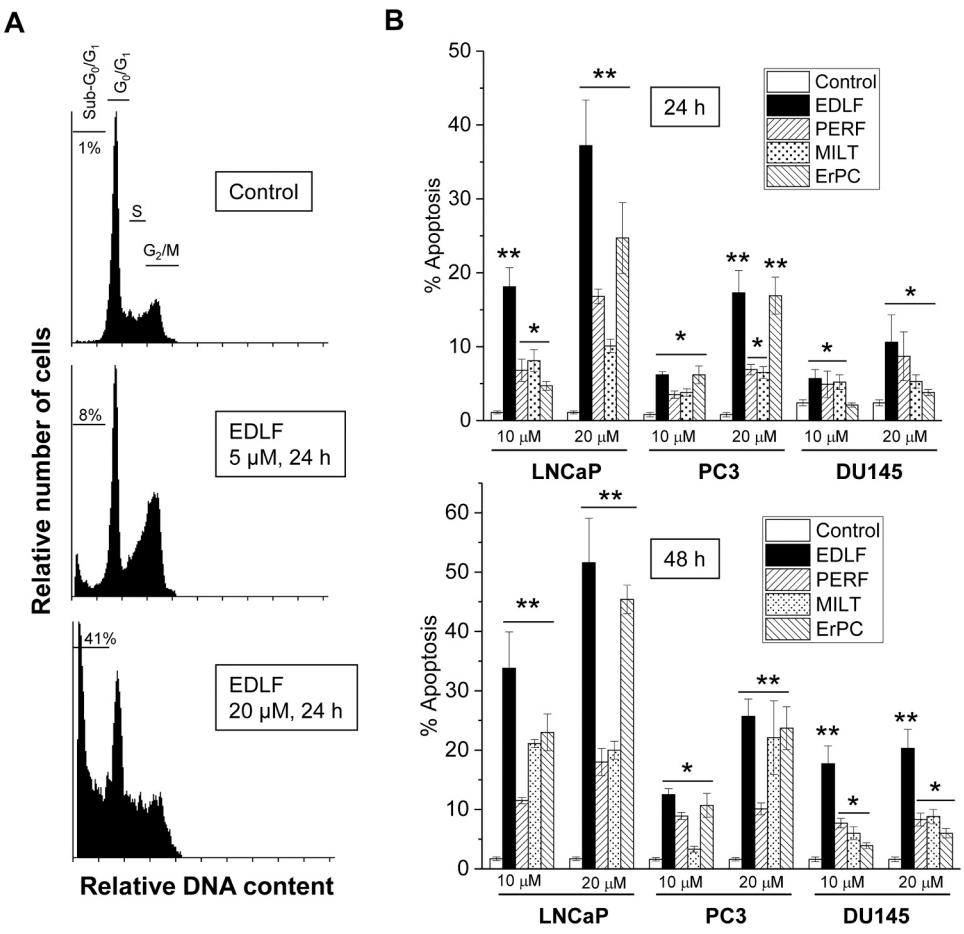

Fig. 2. Induction of apoptosis by edelfosine and additional APLs in human prostate cancer cells. A. Flow cytometry cell cycle profiles of LNCaP cells in untreated (*Control*) and treated with 5 and 20 μM edelfosine for 24 and 48 h. The distinct cell cycle phases, as well as the percentage of cells in the sub-G_0/G_1 region (apoptosis) are indicated. **B.** LNCaP, PC3 and DU145 cells were incubated in the absence (*Control*) or presence of 10 μM and 20 μM of different APLs (edelfosine, EDLF; perifosine, PERF; miltefosine, MILT; erucylphosphocholine, ErPC) for 24 and 48 h, and then the percentage of apoptosis was evaluated as the proportion of cells in the sub-G_0/G_1 region (hypodiploid apoptotic cells). Data shown are means ± SD of at least five independent experiments. Asterisks indicate values that are significantly different from untreated control cells, by comparing untreatead and drug-treated cells. * $P < 0.05$; * * $P < 0.01$.

> erucylphosphocholine ≥ miltefosine ≈ perifosine in their capacity to induce apoptosis in the three human prostate cancer cell lines (Fig. 2B). Interestingly, erucylphosphocholine, the first intravenously applicable APL [63], was also able to promote apoptosis, and this response was particularly high in LNCaP and PC3 cells (Fig. 2B). The erucylphosphocholine analog erufosine behaved similarly, inducing 5.1 ± 0.9% and 25.2 ± 3.5% apoptosis, at 10 and 20 μM respectively, after 24 h treatment and 28.6 ± 3.7% and 44.1 ± 5.2% apoptosis, at 10 and 20 μM respectively, after 48 h treatment in LNCaP cells ($n = 5$). Treatment of LNCaP cells with higher amounts of edelfosine (30 μM) induced 41.7 ± 5.7%, 57.5 ± 6.8% and 77.5 ± 8.3% cell death following 24, 48 and 72 h incubation.

The fluorescent edelfosine analog Et-BDP-ET, previously used to identify the subcellular location of the edelfosine [38,39] accumulated in the ER of the prostate cancer cells (Fig. 3A). CHOP (also known as growth arrest- and DNA damage-inducible gene 153 or GADD153) expression was increased upon edelfosine treatment in all the cell lines, particularly in the LNCaP and DU145 cells (Fig. 3B). Edelfosine induced the cleavage of the caspase-3 and caspase-7 substrate poly(ADP-ribose) polymerase (PARP) into the 85 kDa PARP fragment in all the human prostate cell lines, as a biochemical marker of apoptosis (Fig. 3B). Activated caspase-3 was found in the nuclei of edelfosine-treated prostate cancer cells by confocal microscopy (Fig. 4), further supporting the induction of caspase-dependent apoptosis. In this regard, preincubation with 50 μM cell-permeant pan-caspase inhibitor z-VAD-fmk for 1 h blocked the apoptotic response induced by a 24 h-treatment with 20 μM edelfosine in the three prostate cancer cell lines (38.5 ± 2.3%, 18.2 ± 1.9%, 13.1 ± 1.8% apoptosis in LNCaP, PC3 and DU145 cells treated with 20 μM edelfosine for 24 h in the absence of z-VAD-fmk *versus* 3.9 ± 1.3%, 3.5 ± 0.9%, 3.8 ± 1.2% apoptosis in LNCaP, PC3 and DU145 cells treated with 20 μM edelfosine for 24 h in the presence of z-VAD-fmk, $n = 5$). After a slight and transient inhibition, no persistent AKT inhibition was observed following edelfosine treatment, as assessed by phospho-AKT staining (Fig. 3B). ERK was not inhibited, and, by contrast, a late increase in phosphorylated ERK was observed at protacted incubation times, when apoptosis was already underway (Fig. 3B). A potent autophagic response was triggered in LNCaP and PC3 cells, as assessed by an increase in the level of microtubule-associated protein 1 light chain 3 (LC3)-II form (Fig. 3B and C). The cytosolic form of LC3 (LC3-I), an autophagosomal ortholog of yeast *Atg8*, is modified to generate a LC3-phosphatidylethanolamine conjugate (LC3-II), which is recruited to autophagosomal membranes and used as a marker for autophagy in mammals [64,65]. Autophagy is genetically impaired in DU145 cells because they lack full-length canonical ATG5, a critical autophagy-related protein, due to an alternative splicing of *Atg5* mRNA leading to nonfunctional truncated products [66]. In this context, no LC3-II was detected in edelfosine-treated DU145 cells (Fig. 3B and C).

3.3. Inhibition of autophagy increases edelfosine-induced apoptosis in LNCaP and PC3 cells

Pretreatment of the three prostate cancer cell lines cells with the autophagy inhibitor bafilomycin A1, which inhibits both V-ATPase and autophagosome-lysosome fusion [67], increased the pro-apoptotic activity of edelfosine in LNCaP and PC3, but had no potentiating effect on the autophagy deficient DU145 cells (Fig. 3C).

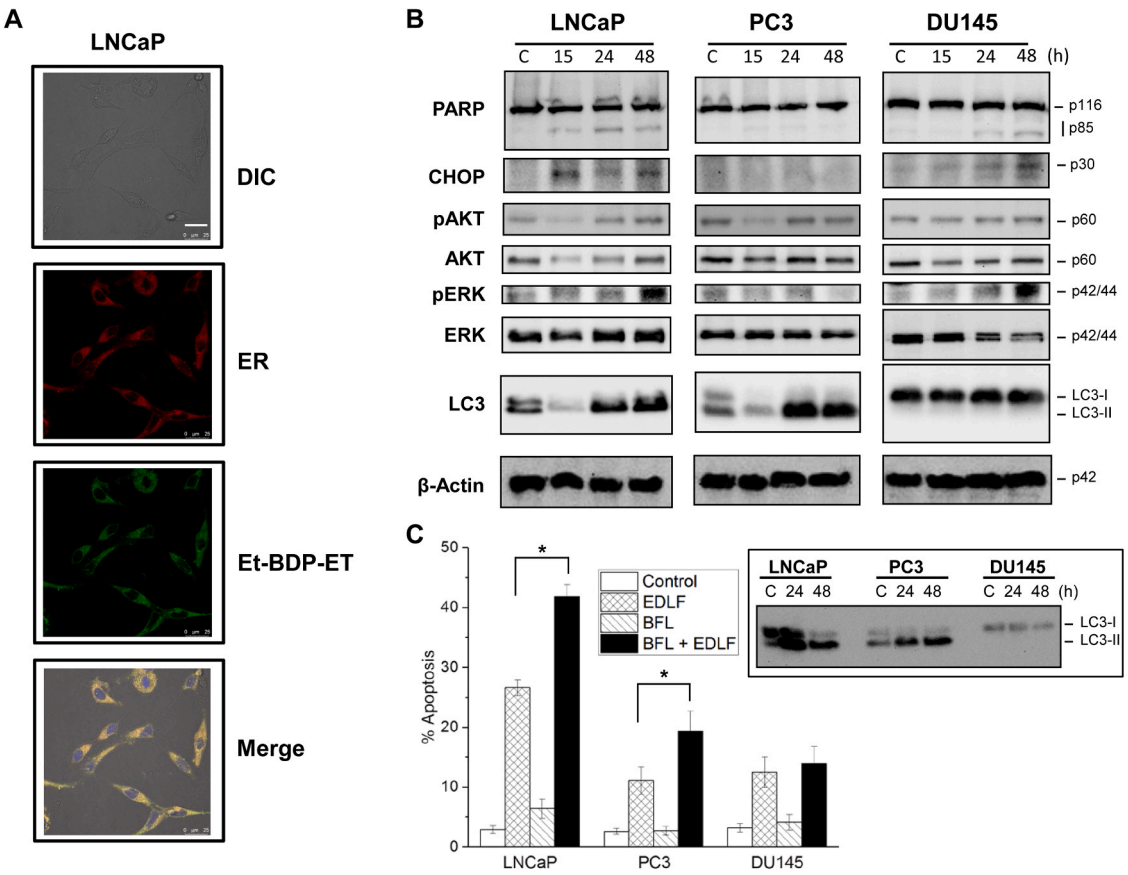

Fig. 3. Drug accumulation in the endoplasmic reticulum, changes in marker proteins following edelfosine treatment, and apoptosis potentiation by preatreatment with bafilomycin A1 in human prostate cancer cells. A. LNCaP cells were labeled overnight at 37 °C for the endoplasmic reticulum (ER) in red using the CellLight ER-RFP BacMam 2.0 reagent, and then the samples were incubated with 20 μM Et-BDP-ET (green fluorescence) for 3 h at 37 °C. Areas of colocalization between the ER and fluorescent analog Et-BDP-ET in the merge panel are yellow. The cells were also stained for nuclei with DAPI (blue fluorescence). The corresponding differential interference contrast (DIC) microscopy images are also shown. Scale bar, 25 μm. The data are representative of three independent experiments. **B.** LNCaP cells were untreated (Control, *C*) or treated with 20 μM edelfosine for the indicated times and analyzed by Western blotting using specific antibodies for the denoted proteins. β-Actin was used as a loading control. Molecular weights (kDa) of every protein are indicated at the right side of each panel. The gels were cropped to show the relevant sections. Data shown are representative of three experiments performed. **C.** LNCaP, PC3 and DU145 cells were preincubated for 1 h in the absence or presence of 15 μM bafilomycin A1 (BFL), and then the cells were incubated in the absence or presence of 20 μM edelfosine (EDLF) for 36 h. Untreated cells (*Control*) were run in parallel. Apoptosis was determined by flow cytometry as the percentage of cells in the sub-G_0/G_1 region. Data shown are means ± SD of five independent experiments. LNCaP, PC3 and DU145 cells were untreated (Control, *C*) or treated with 20 μM edelfosine for the indicated times and analyzed by Western blotting using a specific antibody against LC3 (*inset*). The gels were cropped to show the relevant sections. Asterisks indicate statistically significant differences between the indicated treatments. * $P < 0.05$. Original and uncropped gels related to the Western blot results displayed here are shown in Supplementary Fig. S2.

3.4. In vivo antitumor activity of edelfosine in a prostate cancer xenograft mouse model

We next determined the *in vivo* antitumor activity of orally administered edelfosine using a prostate cancer xenograft mouse model in CB17-severe combined immunodeficient (SCID) mice. Because, tumorigenicity of LNCaP cells has been proved to be rather low in nude mice [56,68], and LNCaP cells have been reported to be less invasive and tumorigenic than DU145 cells [56,69,70], we evaluated the *in vivo* antitumor activity of orally administered edelfosine in a DU145 prostate cancer xenograft animal model, following inoculation of prostate cancer DU145 cells into CB17-SCID mice. In agreement with previous studies in SCID mice [31,32], we found that a daily oral administration of 30 mg/kg edelfosine was well tolerated, with less than 2–3% of body weight loss in non-bearing tumor SCID mice. When tumors were palpable, mice were randomly assigned to two cohorts of 10 mice each, receiving a daily oral administration of 30 mg/kg edelfosine or vehicle (water). Serial caliper measurements were performed weekly to determine the approximate tumor volume until mice were euthanized after an 8-week treatment period (Fig. 5A). Pharmacokinetic studies showed that a daily oral administration of edelfosine for at least 6 days was required to reach a therapeutically relevant drug plasma concentration [71]. The weekly measurements of the subcutaneous tumors with external calipers in drug-treated tumor-bearing mice and untreated control tumor bearing-mice showed that tumors were smaller just after the second week of treatment (Fig. 5A). A kind of plateau in tumor size was reached after the fifth week of drug administration. This could be due in part to the growth arrest of prostate tumor cells induced by edelfosine treatment, followed by the rather slow, but persistent, induction of apoptosis in the prostate tumor cells (Fig. 2). This could lead first to the stoppage of tumor growth and then to tumor regression as it is subtly suggested in Fig. 5A. In fact, a subtle decrease is observed in tumor size after the seventh week of treatment (Fig. 5A). It should also be taken into account that caliper measurements are often affected by errors due to *e.g.* variability in tumor shape, skin thickness and subcutaneous fat layer thickness as well as differences in the compressibility of the tumor [72], and these items could be modified throughout the treatment. A comparison of tumors isolated from untreated control untreated DU145-bearing mice and drug-treated DU145-bearing mice after 8 weeks of treatment showed a potent *in vivo* antitumor activity of

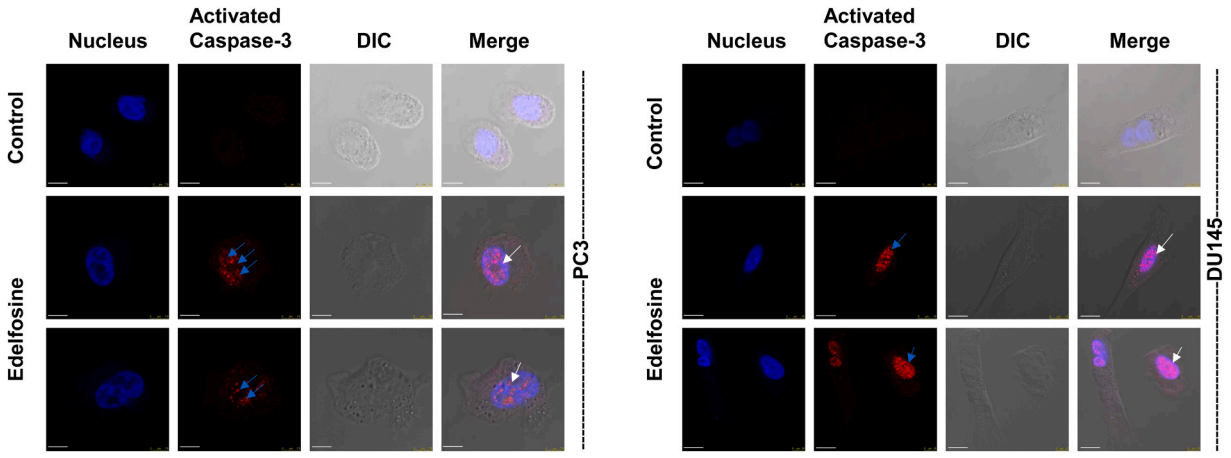

Fig. 4. Confocal microscopy for the expression and localization of activated caspase-3 in prostate cancer cell cells following edelfosine treatment. PC3 and D145 cells were untreated (*Control*) or treated with edelfosine 20 μM for 24 h. Following edelfosine treatment, activated caspase-3 localization was analyzed by confocal microscopy, and colocalized with the nuclei stained in blue with DAPI (arrows). Images shown are representative of three independent experiments. Scale bars, 7.5 μm (PC3) and 10 μm (DU145).

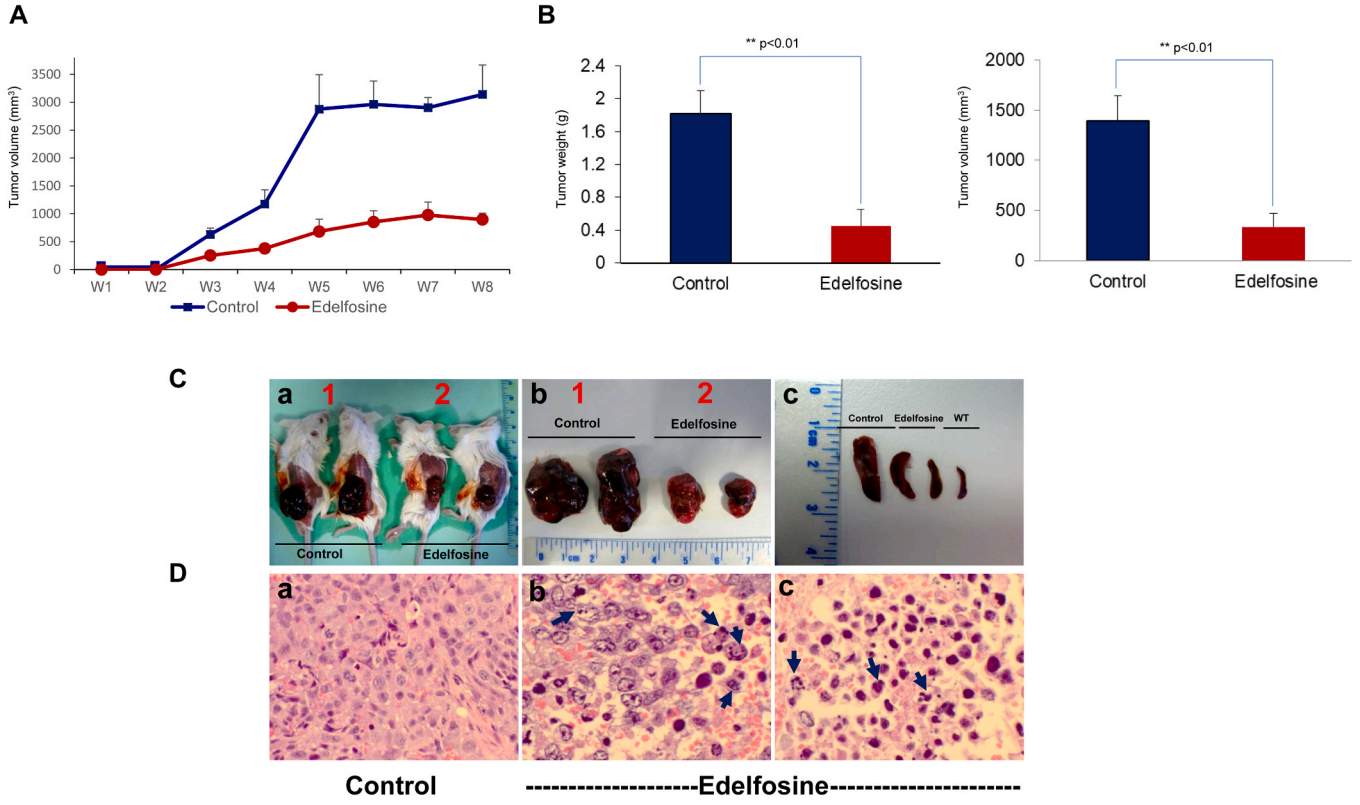

Fig. 5. *In vivo* antitumor activity of edelfosine in human DU145 xenografts. A. CB17-SCID mice were inoculated subcutaneously with DU145 cells. Oral administration of edelfosine (30 mg/kg, once-daily dosing regimen) and water vehicle (*Control*) started in parallel after the development of a palpable tumor in tumor-bearing mice ($n = 10$). Caliper measurements of each tumor were carried out weekly (W) at the indicated times. Data shown are means ± SD ($n = 10$). **B**. After completion of the *in vivo* assays, control drug-free mice and animals treated with 30 mg/kg edelfosine were euthanized and isolated tumor weight and volume were measured. Data shown are means ± SD ($n = 10$). * *, $P < 0.01$, Student's *t*-test. **C**. Significant tumor growth inhibition was observed after edelfosine treatment in DU145-bearing SCID mice. Two representative DU145-bearing SCID mice control and edelfosine-treated mice, out of ten tested, and the corresponding isolated tumors from drug-free DU145-bearing mice (*Control*; a1, b1) and edelfosine-treated groups (*Edelfosine*; a2, b2), are shown. Spleens isolated from representative drug-free DU145-bearing mice (*Control*), edelfosine-treated mice (*Edelfosine*) and untreated non-tumor-bearing wild-type mice (*WT*) are shown (c). **D**. Edelfosine induces apoptosis in prostate cancer tumor xenografts. Light microscopic examination with H&E staining (x200 magnification) of xenograft tumors were performed in tumor-bearing drug-free SCID mice (*Control*, a) and animals treated with 30 mg/kg edelfosine (*Edelfosine*, b, c). Tissue sections of tumors stained with H&E showed the presence of irregular cells with hypereosinophilic cytoplasm and nuclear karyorrhexis and/or pyknosis (arrow), indicative of cell death by apoptosis, following edelfosine treatment (b, c).

edelfosine, with a reduction of 75% and 77% in tumor weight and volume, respectively (Fig. 5B and C). No apparent toxicity was observed in mice treated with edelfosine after necropsy analysis. Likewise, no significant differences changes in body weight between drug-treated and untreated control animals were detected (less than 3% of body weight loss in drug-treated *vs.* untreated control cohorts). Interestingly, spleen was enlarged in the untreated tumor-bearing immunodeficient mice when compared with that of untreated wild-type mice, while edelfosine treatment reduced this enlargement (Fig. 5C). Splenomegaly is commonly seen in tumor cell transplantable models [73,74]. Examination of H&E sections of tumors indicated that samples from edelfosine-treated mice showed the presence of irregular cells with hypereosinophilic cytoplasm and nuclear karyorrhexis and/or pyknosis, characteristic of apoptotic cell death (Fig. 5D). Quantitation of the percentage of prostate cancer cells showing apoptotic cell death in ten high-powered fields in the prostate cancer xenografts, similar to those illustrated in Fig. 5D, indicated that edelfosine treatment induced 19.7 $\pm$ 6.5% apoptosis *versus* 1.8 $\pm$ 0.5% in untreated tumor-bearing mice ($n = 10$).

4. Discussion

Here we demonstrate the antitumor activity of the ether lipid edelfosine against prostate cancer through both *in vitro* and *in vivo* approaches. Oral administration of edelfosine was able to inhibit tumor progression in both transgenic and xenograft animal models, thus demonstrating a sound antitumor activity of this ether lipid against prostate cancer. Edelfosine pro-apoptotic activity was higher than that displayed by other clinically relevant APLs, such as perifosine, used in clinical trials against a variety of tumors [52,75], and miltefosine, currently used as a topical treatment of cutaneous metastases in breast cancer [76], and as the first oral antileishmanial agent, constituting a breakthrough in leishmaniasis treatment [77,78]. In this regard, edelfosine has also been shown to be an effective drug in killing different species of *Leishmania* parasites in both *in vitro* and *in vivo* assays, being more potent than miltefosine [79,80]. Importantly, we found that edelfosine was able to inhibit tumor progression in two different animal models for prostate cancer, involving transgenic and xenograft approaches. It is interesting to note that oral administration was able to inhibit tumor progression in a DU145-xenograft mice model, despite DU145 cells were less sensitive to undergo apoptosis following edelfosine treatment *in vitro* than other prostate cancer cell lines, such as LNCaP cells. Furthermore, we found that edelfosine induced about 20% apoptosis in histological analyses of DU145 xenograft tumors, using standard H&E stains and apoptotic morphological criteria. In this regard, it is tempting to suggest that the percentage of apoptotic cells could be even higher, because measurements of apoptosis in histological sections following morphological criteria may underestimate the rate of apoptosis by 2-fold to 3-fold [81,82]. We also found that edelfosine ameliorated the increase in spleen size as compared to untreated prostate tumor-bearing mice in the prostate cancer xenograft experiments. The spleen is the most important immune organ in the body, containing innate and adaptative immune cells and playing a major role in the antitumor immune response [83]. Thus, it contains both tumor-suppressive cells, including natural killer (NK) cells and activated T cells, and tumor-promoting cells, such as regulatory T cells (Tregs), myeloid-derived suppressor cells (MDSCs), tumor-associated macrophages (TAMs) and tumor-associated neutrophils (TANs), which could lead to a paradoxical effect in tumor immunology, from a putative elimination of nascent tumors at the early stages to tumor immune tolerance at later stages of tumor progression [74,83–86]. Development of splenomegaly has been largely reported in xenograft-harboring immunodeficient mice, which was reduced following drug treatment [87–90]. Although the dynamics of the spleen during tumor progression remains incompletely understood, it has been shown a correlation between reduction of splenomegaly and reduction of tumor size [87–92]. Because mature lymphoid differentiation is specifically impaired in immunodeficient SCID mice whereas myeloid differentiation is not affected [93,94], a major role of certain myeloid cells in the spleen during tumor progression could be tentatively suggested [83,91,95]. The transgenic MPAKT model involves PIN through prostate restricted AKT activation [41]. Edelfosine inhibits AKT by displacing AKT and regulatory proteins from lipid rafts in mantle cell lymphoma [96]. Edelfosine has been previously found to exert a dose-response decrease in AKT activity, without affecting AKT total expression, and inhibited the expression of androgen receptor, which was associated with an increase in the expression of activating transcription factor 3 (ATF3) in LNCaP cells, an ER stress response gene [97,98] and a negative regulator of androgen receptor [99], leading to the induction of apoptosis in LNCaP cells, as assessed by Annexin V staining [100]. Previous reports have shown that the APL perifosine, acting as an AKT inhibitor [101–103], has a modest single-agent clinical activity in phase II clinical trials in patients with biochemically recurrent, hormone-sensitive prostate cancer [104]. Here, we found that edelfosine was more active than perifosine in promoting apoptosis, and was unable to promote a persistent AKT inhibition in the different three prostate cell lines used in the present study. Although edelfosine was more effective in killing the PTEN-null LNCaP cell line than the PTEN-positive DU145 cell line, oral administration of the ether lipid in the DU145 xenograft model for prostate cancer led to a dramatic tumor regression. DU145 cells are androgen-independent, and androgen-refractory prostate cancer cells, as compared with androgen-sensitive ones, are more resistant to chemotherapies [66].

Taken together, the above results suggest the major contribution of additional factors, apart from AKT inhibition, in edelfosine-mediated apoptosis in prostate cancer cells. In this regard, edelfosine has been reported to accumulate in the ER and promote apoptosis following a persistent ER stress response in different solid tumors [30], including pancreatic cancer and Ewing's sarcoma [31,32]. Edelfosine has been recently found to promote apoptosis in human pancreatic cancer stem cells through its accumulation in ER and subsequent induction of ER stress [39]. Here, we have found that edelfosine accumulated in the ER of prostate cancer cells and increased the expression of CHOP, a marker for ER stress response associated to ER-stress-mediated apoptosis [30–32]. Because the cell lines used in this study show different androgen dependency as well as p53 and PTEN status, the results reported here suggest that targeting ER can be a novel approach for the treatment of prostate cancer, independently of PTEN expression, androgen dependency or p53 status. In addition to their regulation by hormones, prostate cancer cells are highly secretory [35]. The ER is the organelle responsible for the synthesis and maturation of proteins that are destined for the secretory pathways, and has become a promising target in tumor chemotherapy [33,105]. In this context, recent reports have also shown that different agents display antitumor effects against prostate cancer cells through an ER stress response [106–110]. Furthermore, ER stress inhibits androgen receptor expression in luminal androgen receptor triple-negative breast cancer and prostate cancer [111]. Thus, the accumulation of edelfosine in the ER of prostate cancer cells and the ability of this antitumor ether lipid to promote apoptosis in different prostate cancer cell lines, as well as to inhibit prostate cancer progression in transgenic and xenograft animal models for prostate cancer, suggest that edelfosine could be a promising drug in the treatment of prostate cancer. Furthermore, oral administration of effective edelfosine doses did not show apparent toxicity in the herein reported *in vivo* assays, in agreement with previous reports using free [24,25,31,32,34] and encapsulated edelfosine in nanoparticles [71,112,113]. Taken together, the results reported here provide the proof of concept for the anti-prostate cancer efficacy of edelfosine, and warrant continued research and clinical evaluation of the effectiveness of edelfosine in future clinical trials.

5. Conclusions

In summary, the herein reported *in vitro* and *in vivo* evidence demonstrates an effective antitumor activity of the ether lipid edelfosine against prostate cancer, regardless of androgen dependency or p53 and PTEN status. Our results indicate that edelfosine is the most potent alkylphospholipid analog in inducing apoptosis, and that endoplasmic reticulum can be effectively targeted by edelfosine to promote cell death in prostate tumor cells. Oral administration of edelfosine induced significant tumor regression in transgenic and xenograft animal prostate cancer models without any apparent toxicity, highlighting its efficacy and safety. Edelfosine could be a valuable novel drug in the treatment of prostate cancer and its action can be potentiated by autophagy inhibition. This study also highlights the role of the endoplasmic reticulum as a novel therapeutic target for the treatment of prostate cancer.

Funding

This work was supported by grant PID2020-119656RB-I00 funded by MCIN/AEI/10.13039/501100011033 from the Spanish Ministry of Science and Innovation (Agencia Estatal de Investigación), as well as by grants from the Spanish Ministry of Science, Innovation and Universities (SAF2017-89672-R, and SAF2014-59716-R).

CRediT authorship contribution statement

EL-Habib Dakir: Conceptualization, Investigation, Methodology, Formal analysis, Writing – review & editing. **Consuelo Gajate:** Conceptualization, Investigation, Methodology, Formal analysis, Writing – review & editing. **Faustino Mollinedo:** Conceptualization, Investigation, Formal analysis, Funding acquisition, Writing – original draft, Writing – review & editing. All the authors have read and approved the final version of the manuscript.

Declaration of Competing Interest

The authors declare that they have no conflict of interest.

Acknowledgements

We thank the technical assistance of Ramón Romero-Varo (CIB – Margarita Salas, Madrid, Spain). F.M. belongs to the Spanish National Research Council (CSIC)'s Cancer Hub.

Appendix A. Supporting information

Supplementary data associated with this article can be found in the online version at doi:10.1016/j.biopha.2023.115436.

References

[1] H. Sung, J. Ferlay, R.L. Siegel, M. Laversanne, I. Soerjomataram, A. Jemal, F. Bray, Global cancer statistics 2020: Globocan estimates of incidence and mortality worldwide for 36 cancers in 185 countries, CA Cancer J. Clin. 71 (2021) 209–249.

[2] P.F. Pinsky, G. Andriole, E.D. Crawford, D. Chia, B.S. Kramer, R. Grubb, R. Greenlee, J.K. Gohagan, Prostate-specific antigen velocity and prostate cancer Gleason grade and stage, Cancer 109 (2007) 1689–1695.

[3] J. Valero, P. Peleteiro, I. Henriquez, A. Conde, T. Piquer, A. Lozano, C.C. Soler, J. Munoz, A. Illescas, J. Jove, M.M. Flores, J. Baquedano, P. Diezhandino, R.P. de Celis, E.H. Pardo, P. Samper, I. Villoslada, M. Eguiguren, V. Millan, Age, Gleason score, and PSA are important prognostic factors for survival in metastatic castration-resistant prostate cancer. Results of the URONCOR group (uro-oncological tumors) of the Spanish society of radiation oncology (SEOR), Clin. Transl. Oncol. 22 (2020) 1378–1389.

[4] H.G. Welch, D.H. Gorski, P.C. Albertsen, Trends in metastatic breast and prostate cancer, New Engl. J. Med. 374 (2016) 596.

[5] L. Bubendorf, A. Schopfer, U. Wagner, G. Sauter, H. Moch, N. Willi, T.C. Gasser, M.J. Mihatsch, Metastatic patterns of prostate cancer: an autopsy study of 1,589 patients, Hum. Pathol. 31 (2000) 578–583.

[6] M. Norgaard, A.O. Jensen, J.B. Jacobsen, K. Cetin, J.P. Fryzek, H.T. Sorensen, Skeletal related events, bone metastasis and survival of prostate cancer: a population based cohort study in Denmark (1999 to 2007), J. Urol. 184 (2010) 162–167.

[7] M.S. Litwin, H.J. Tan, The diagnosis and treatment of prostate cancer: a review, JAMA 317 (2017) 2532–2542.

[8] A.J. Evans, Treatment effects in prostate cancer, Mod. Pathol. 31 (2018) S110–121.

[9] U. Swami, T.R. McFarland, R. Nussenzveig, N. Agarwal, Advanced prostate cancer: Treatment advances and future directions, Trends Cancer 6 (2020) 702–715.

[10] I.B. Riaz, C.J. Sweeney, The role of chemotherapy in metastatic prostate cancer, Curr. Opin. Urol. 32 (2022) 292–301.

[11] N. Sayegh, U. Swami, N. Agarwal, Recent advances in the management of metastatic prostate cancer, JCO Oncol. Pract. 18 (2022) 45–55.

[12] O. Sartor, J. de Bono, K.N. Chi, K. Fizazi, K. Herrmann, K. Rahbar, S.T. Tagawa, L. T. Nordquist, N. Vaishampayan, G. El-Haddad, C.H. Park, T.M. Beer, A. Armour, W.J. Perez-Contreras, M. DeSilvio, E. Kpamegan, G. Gericke, R.A. Messmann, M. J. Morris, B.J. Krause, Lutetium-177-PSMA-617 for metastatic castration-resistant prostate cancer, New Engl. J. Med. 385 (2021) 1091–1103.

[13] S. Tonyali, H.B. Haberal, E. Sogutdelen, Toxicity, adverse events, and quality of life associated with the treatment of metastatic castration-resistant prostate cancer, Curr. Urol. 10 (2017) 169–173.

[14] C. Gajate, F. Mollinedo, Biological activities, mechanisms of action and biomedical prospect of the antitumor ether phospholipid ET-18-OCH_3 (edelfosine), a proapoptotic agent in tumor cells, Curr. Drug Metab. 3 (2002) 491–525.

[15] F. Mollinedo, C. Gajate, S. Martin-Santamaria, F. Gago, ET-18-OCH_3 (edelfosine): a selective antitumour lipid targeting apoptosis through intracellular activation of Fas/CD95 death receptor, Curr. Med. Chem. 11 (2004) 3163–3184.

[16] F. Mollinedo, Editorial: Antitumor alkylphospholipid analogs: a promising and growing family of synthetic cell membrane-targeting molecules for cancer treatment, Anticancer Agents Med. Chem. 14 (2014) 495–498.

[17] P.A. Jaffres, C. Gajate, A.M. Bouchet, H. Couthon-Gourves, A. Chantome, M. Potier-Cartereau, P. Besson, P. Bougnoux, F. Mollinedo, C. Vandier, Alkyl ether lipids, ion channels and lipid raft reorganization in cancer therapy, Pharmacol. Ther. 165 (2016) 114–131.

[18] F. Mollinedo, J.L. Fernandez-Luna, C. Gajate, B. Martin-Martin, A. Benito, R. Martinez-Dalmau, M. Modolell, Selective induction of apoptosis in cancer cells by the ether lipid ET-18-OCH_3 (edelfosine): Molecular structure requirements, cellular uptake, and protection by Bcl-2 and Bcl-X_L, Cancer Res. 57 (1997) 1320–1328.

[19] F. Mollinedo, Antitumor ether lipids: proapoptotic agents with multiple therapeutic indications, Expert Opin. Ther. Pat. 17 (2007) 385–405.

[20] C. Gajate, F. Mollinedo, The antitumor ether lipid ET-18-OCH_3 induces apoptosis through translocation and capping of Fas/CD95 into membrane rafts in human leukemic cells, Blood 98 (2001) 3860–3863.

[21] C. Gajate, E. Del Canto-Janez, A.U. Acuna, F. Amat-Guerri, E. Geijo, A.M. Santos-Beneit, R.J. Veldman, F. Mollinedo, Intracellular triggering of Fas aggregation and recruitment of apoptotic molecules into Fas-enriched rafts in selective tumor cell apoptosis, J. Exp. Med. 200 (2004) 353–365.

[22] F. Mollinedo, C. Gajate, Fas/CD95 death receptor and lipid rafts: New targets for apoptosis-directed cancer therapy, Drug Resist Updat 9 (2006) 51–73.

[23] C. Gajate, F. Mollinedo, Edelfosine and perifosine induce selective apoptosis in multiple myeloma by recruitment of death receptors and downstream signaling molecules into lipid rafts, Blood 109 (2007) 711–719.

[24] F. Mollinedo, J. de la Iglesia-Vicente, C. Gajate, A. Estella-Hermoso de Mendoza, J.A. Villa-Pulgarin, M.A. Campanero, M.J. Blanco-Prieto, Lipid raft-targeted therapy in multiple myeloma, Oncogene 29 (2010) 3748–3757.

[25] F. Mollinedo, J. de la Iglesia-Vicente, C. Gajate, A. Estella-Hermoso de Mendoza, J.A. Villa-Pulgarin, M. de Frias, G. Roue, J. Gil, D. Colomer, M.A. Campanero, M. J. Blanco-Prieto, In vitro and in vivo selective antitumor activity of edelfosine against mantle cell lymphoma and chronic lymphocytic leukemia involving lipid rafts, Clin. Cancer Res. 16 (2010) 2046–2054.

[26] C. Gajate, F. Mollinedo, Lipid rafts, endoplasmic reticulum and mitochondria in the antitumor action of the alkylphospholipid analog edelfosine, Anticancer Agents Med. Chem. 14 (2014) 509–527.

[27] C. Gajate, F. Mollinedo, Lipid raft-mediated Fas/CD95 apoptotic signaling in leukemic cells and normal leukocytes and therapeutic implications, J. Leukoc. Biol. 98 (2015) 739–759.

[28] F. Mollinedo, C. Gajate, Lipid rafts as signaling hubs in cancer cell survival/death and invasion: Implications in tumor progression and therapy, J. Lipid Res. 61 (2020) 611–635.

[29] F. Mollinedo, C. Gajate, Clusters of apoptotic signaling molecule-enriched rafts, CASMERs: Membrane platforms for protein assembly in Fas/CD95 signaling and targets in cancer therapy, Biochem. Soc. Trans. 50 (2022) 1105–1118.

[30] T. Nieto-Miguel, R.I. Fonteriz, L. Vay, C. Gajate, S. Lopez-Hernandez, F. Mollinedo, Endoplasmic reticulum stress in the proapoptotic action of edelfosine in solid tumor cells, Cancer Res. 67 (2007) 10368–10378.

[31] C. Gajate, M. Matos-da-Silva, H. Dakir el, R.I. Fonteriz, J. Alvarez, F. Mollinedo, Antitumor alkyl-lysophospholipid analog edelfosine induces apoptosis in pancreatic cancer by targeting endoplasmic reticulum, Oncogene 31 (2012) 2627–2639.

[32] X. Bonilla, H. Dakir el, F. Mollinedo, C. Gajate, Endoplasmic reticulum targeting in Ewing's sarcoma by the alkylphospholipid analog edelfosine, Oncotarget 6 (2015) 14596–14613.

[33] F. Mollinedo, C. Gajate, Direct endoplasmic reticulum targeting by the selective alkylphospholipid analog and antitumor ether lipid edelfosine as a therapeutic approach in pancreatic cancer, Cancers 13 (2021) 4173.
[34] F. Mollinedo, C. Gajate, A.I. Morales, E. del Canto-Janez, N. Justies, F. Collia, J. V. Rivas, M. Modolell, A. Iglesias, Novel anti-inflammatory action of edelfosine lacking toxicity with protective effect in experimental colitis, J. Pharm. Exp. Ther. 329 (2009) 439–449.
[35] Y. Erzurumlu, P. Ballar, Androgen mediated regulation of endoplasmic reticulum-associated degradation and its effects on prostate cancer, Sci. Rep. 7 (2017) 40719.
[36] M. Korcek, M. Sekeresova, A.V. Makarevich, H. Gavurova, L. Olexikova, J. Pivko, L. Barreto, Morphological and functional alterations of the prostate tissue during clinical progression in hormonally-naive, hormonally-treated and castration-resistant patients with metastatic prostate cancer, Oncol. Lett. 20 (2020) 201.
[37] C. Gajate, R.I. Fonteriz, C. Cabaner, G. Alvarez-Noves, Y. Alvarez-Rodriguez, M. Modolell, F. Mollinedo, Intracellular triggering of Fas, independently of FasL, as a new mechanism of antitumor ether lipid-induced apoptosis, Int J. Cancer 85 (2000) 674–682.
[38] F. Mollinedo, M. Fernandez, V. Hornillos, J. Delgado, F. Amat-Guerri, A.U. Acuna, T. Nieto-Miguel, J.A. Villa-Pulgarin, C. Gonzalez-Garcia, V. Cena, C. Gajate, Involvement of lipid rafts in the localization and dysfunction effect of the antitumor ether phospholipid edelfosine in mitochondria, Cell Death Dis. 2 (2011), e158.
[39] C. Gajate, O. Gayet, N.A. Fraunhoffer, J. Iovanna, N. Dusetti, F. Mollinedo, Induction of apoptosis in human pancreatic cancer stem cells by the endoplasmic reticulum-targeted alkylphospholipid analog edelfosine and potentiation by autophagy inhibition, Cancers 13 (2021) 6124.
[40] C. Gajate, F. Mollinedo, Lipid raft isolation by sucrose gradient centrifugation and visualization of raft-located proteins by fluorescence microscopy: the use of combined techniques to assess Fas/CD95 location in rafts during apoptosis triggering, Methods Mol. Biol. 2187 (2021) 147–186.
[41] P.K. Majumder, J.J. Yeh, D.J. George, P.G. Febbo, J. Kum, Q. Xue, R. Bikoff, H. Ma, P.W. Kantoff, T.R. Golub, M. Loda, W.R. Sellers, Prostate intraepithelial neoplasia induced by prostate restricted Akt activation: The MPAKT model, Proc. Natl. Acad. Sci. USA 100 (2003) 7841–7846.
[42] N.M. Greenberg, F. DeMayo, M.J. Finegold, D. Medina, W.D. Tilley, J.O. Aspinall, G.R. Cunha, A.A. Donjacour, R.J. Matusik, J.M. Rosen, Prostate cancer in a transgenic mouse, Proc. Natl. Acad. Sci. USA 92 (1995) 3439–3443.
[43] M. Ittmann, J. Huang, E. Radaelli, P. Martin, S. Signoretti, R. Sullivan, B.W. Simons, J.M. Ward, B.D. Robinson, G.C. Chu, M. Loda, G. Thomas, A. Borowsky, R.D. Cardiff, Animal models of human prostate cancer: The consensus report of the New York meeting of the mouse models of human cancers consortium prostate pathology committee, Cancer Res 73 (2013) 2718–2736.
[44] S. Saranyutanon, S.K. Deshmukh, S. Dasgupta, S. Pai, S. Singh, A.P. Singh, Cellular and molecular progression of prostate cancer: Models for basic and preclinical research, Cancers 12 (2020) 2651.
[45] E.H. Dakir, L. Feigenbaum, R.I. Linnoila, Constitutive expression of human keratin 14 gene in mouse lung induces premalignant lesions and squamous differentiation, Carcinogenesis 29 (2008) 2377–2384.
[46] A. Di Cristofano, B. Pesce, C. Cordon-Cardo, P.P. Pandolfi, *Pten* is essential for embryonic development and tumour suppression, Nat. Genet. 19 (1998) 348–355.
[47] D.M. Euhus, C. Hudd, M.C. LaRegina, F.E. Johnson, Tumor measurement in the nude mouse, J. Surg. Oncol. 31 (1986) 229–234.
[48] M.M. Tomayko, C.P. Reynolds, Determination of subcutaneous tumor size in athymic (nude) mice, Cancer Chemother. Pharm. 24 (1989) 148–154.
[49] V.G. Doddawad, Histopathological analysis of apoptotic cell count and its role in oral lichen planus, J. Oral. Maxillofac. Pathol. 18 (2014) 42–45.
[50] S.A. Elmore, D. Dixon, J.R. Hailey, T. Harada, R.A. Herbert, R.R. Maronpot, T. Nolte, J.E. Rehg, S. Rittinghausen, T.J. Rosol, H. Satoh, J.D. Vidal, C.L. Willard-Mack, D.M. Creasy, Recommendations from the INHAND apoptosis/necrosis working group, Toxicol. Pathol. 44 (2016) 173–188.
[51] W.J. van Blitterswijk, M. Verheij, Anticancer alkylphospholipids: mechanisms of action, cellular sensitivity and resistance, and clinical prospects, Curr. Pharm. Des. 14 (2008) 2061–2074.
[52] W.J. van Blitterswijk, M. Verheij, Anticancer mechanisms and clinical application of alkylphospholipids, Biochim Biophys. Acta 1831 (2013) 663–674.
[53] A. Pachioni Jde, J.G. Magalhaes, E.J. Lima, M. Bueno Lde, J.F. Barbosa, M.M. de Sa, C.O. Rangel-Yagui, Alkylphospholipids - a promising class of chemotherapeutic agents with a broad pharmacological spectrum, J. Pharm. Pharm. Sci. 16 (2013) 742–759.
[54] A. Kostadinova, T. Topouzova-Hristova, A. Momchilova, R. Tzoneva, M.R. Berger, Antitumor lipids–structure, functions, and medical applications, Adv. Protein Chem. Struct. Biol. 101 (2015) 27–66.
[55] P. Rios-Marco, C. Marco, X. Galvez, J.M. Jimenez-Lopez, M.P. Carrasco, Alkylphospholipids: An update on molecular mechanisms and clinical relevance, Biochim. Biophys. Acta Biomembr. 1859 (2017) 1657–1667.
[56] X. Wu, S. Gong, P. Roy-Burman, P. Lee, Z. Culig, Current mouse and cell models in prostate cancer research, Endocr. Relat. Cancer 20 (2013) R155–170.
[57] D. Cunningham, Z. You, In vitro and in vivo model systems used in prostate cancer research, J. Biol. Methods 2 (2015) e17.
[58] J.S. Horoszewicz, S.S. Leong, E. Kawinski, J.P. Karr, H. Rosenthal, T.M. Chu, E. A. Mirand, G.P. Murphy, LNCaP model of human prostatic carcinoma, Cancer Res. 43 (1983) 1809–1818.
[59] C. Abate-Shen, F. Nunes, de Almeida, Establishment of the LNCaP cell line - the dawn of an era for prostate cancer research, Cancer Res. 82 (2022) 1689–1691.
[60] K.R. Stone, D.D. Mickey, H. Wunderli, G.H. Mickey, D.F. Paulson, Isolation of a human prostate carcinoma cell line (DU 145), Int. J. Cancer 21 (1978) 274–281.
[61] M.E. Kaighn, K.S. Narayan, Y. Ohnuki, J.F. Lechner, L.W. Jones, Establishment and characterization of a human prostatic carcinoma cell line (PC-3), Investig. Urol. 17 (1979) 16–23.
[62] S. Tai, Y. Sun, J.M. Squires, H. Zhang, W.K. Oh, C.Z. Liang, J. Huang, PC3 is a cell line characteristic of prostatic small cell carcinoma, Prostate 71 (2011) 1668–1679.
[63] B. Erdlenbruch, V. Jendrossek, A. Gerriets, F. Vetterlein, H. Eibl, M. Lakomek, Erucylphosphocholine: pharmacokinetics, biodistribution and CNS-accumulation in the rat after intravenous administration, Cancer Chemother. Pharmacol. 44 (1999) 484–490.
[64] R. Garcia-Navas, M. Munder, F. Mollinedo, Depletion of L-arginine induces autophagy as a cytoprotective response to endoplasmic reticulum stress in human T lymphocytes, Autophagy 8 (2012) 1557–1576.
[65] L. Li, M. Tong, Y. Fu, F. Chen, S. Zhang, H. Chen, X. Ma, D. Li, X. Liu, Q. Zhong, Lipids and membrane-associated proteins in autophagy, Protein Cell 12 (2021) 520–544.
[66] D.Y. Ouyang, L.H. Xu, X.H. He, Y.T. Zhang, L.H. Zeng, J.Y. Cai, S. Ren, Autophagy is differentially induced in prostate cancer LNCaP, DU145 and PC-3 cells via distinct splicing profiles of ATG5, Autophagy 9 (2013) 20–32.
[67] C. Mauvezin, T.P. Neufeld, Bafilomycin A1 disrupts autophagic flux by inhibiting both V-ATPase-dependent acidification and Ca-P60A/SERCA-dependent autophagosome-lysosome fusion, Autophagy 11 (2015) 1437–1438.
[68] W. Liu, Y. Zhu, L. Ye, Y. Wang, Establishment of an orthotopic prostate cancer xenograft mouse model using microscope-guided orthotopic injection of LNCaP cells into the dorsal lobe of the mouse prostate, BMC Cancer 22 (2022) 173.
[69] G.J. Klarmann, E.M. Hurt, L.A. Mathews, X. Zhang, M.A. Duhagon, T. Mistree, S. B. Thomas, W.L. Farrar, Invasive prostate cancer cells are tumor initiating cells that have a stem cell-like genomic signature, Clin. Exp. Metastasis 26 (2009) 433–446.
[70] F. Crea, E.M. Hurt, L.A. Mathews, S.M. Cabarcas, L. Sun, V.E. Marquez, R. Danesi, W.L. Farrar, Pharmacologic disruption of polycomb repressive complex 2 inhibits tumorigenicity and tumor progression in prostate cancer, Mol. Cancer 10 (2011) 40.
[71] A. Estella-Hermoso de Mendoza, M.A. Campanero, J. de la Iglesia-Vicente, C. Gajate, F. Mollinedo, M.J. Blanco-Prieto, Antitumor alkyl ether lipid edelfosine: tissue distribution and pharmacokinetic behavior in healthy and tumor-bearing immunosuppressed mice, Clin. Cancer Res. 15 (2009) 858–864.
[72] M.M. Jensen, J.T. Jorgensen, T. Binderup, A. Kjaer, Tumor volume in subcutaneous mouse xenografts measured by microCT is more accurate and reproducible than determined by 18F-FDG-microPET or external caliper, BMC Med Imaging 8 (2008) 16.
[73] D.I. Gabrilovich, S. Ostrand-Rosenberg, V. Bronte, Coordinated regulation of myeloid cells by tumours, Nat. Rev. Immunol. 12 (2012) 253–268.
[74] V. Bronte, M.J. Pittet, The spleen in local and systemic regulation of immunity, Immunity 39 (2013) 806–818.
[75] T.J. Kaley, K.S. Panageas, E.I. Pentsova, I.K. Mellinghoff, C. Nolan, I. Gavrilovic, L.M. DeAngelis, L.E. Abrey, E.C. Holland, A. Omuro, M.E. Lacouture, E. Ludwig, A.B. Lassman, Phase I clinical trial of temsirolimus and perifosine for recurrent glioblastoma, Ann. Clin. Transl. Neurol. 7 (2020) 429–436.
[76] R. Leonard, J. Hardy, G. van Tienhoven, S. Houston, P. Simmonds, M. David, J. Mansi, Randomized, double-blind, placebo-controlled, multicenter trial of 6% miltefosine solution, a topical chemotherapy in cutaneous metastases from breast cancer, J. Clin. Oncol. 19 (2001) 4150–4159.
[77] S. Sundar, T.K. Jha, C.P. Thakur, S.K. Bhattacharya, M. Rai, Oral miltefosine for the treatment of Indian visceral leishmaniasis, Trans. R. Soc. Trop. Med Hyg. 100 (1) (2006) S26–33.
[78] S. Sundar, A. Singh, M. Rai, V.K. Prajapati, A.K. Singh, B. Ostyn, M. Boelaert, J. C. Dujardin, J. Chakravarty, Efficacy of miltefosine in the treatment of visceral leishmaniasis in India after a decade of use, Clin. Infect. Dis. 55 (2012) 543–550.
[79] R.E. Varela-M, J.A. Villa-Pulgarin, E. Yepes, I. Muller, M. Modolell, D.L. Munoz, S. M. Robledo, C.E. Muskus, J. Lopez-Aban, A. Muro, I.D. Velez, F. Mollinedo, *In vitro* and *in vivo* efficacy of ether lipid edelfosine against *Leishmania spp.* and SbV-resistant parasites, PLoS Negl. Trop. Dis. 6 (2012), e1612.
[80] J.A. Villa-Pulgarin, C. Gajate, J. Botet, A. Jimenez, N. Justies, R.E. Varela-M, A. Cuesta-Marban, I. Muller, M. Modolell, J.L. Revuelta, F. Mollinedo, Mitochondria and lipid raft-located F_OF_1-ATP synthase as major therapeutic targets in the antileishmanial and anticancer activities of ether lipid edelfosine, PLoS Negl. Trop. Dis. 11 (2017), e0005805.
[81] K.R. Jerome, C. Vallan, R. Jaggi, The TUNEL assay in the diagnosis of graft-versus-host disease: Caveats for interpretation, Pathology 32 (2000) 186–190.
[82] M.M. Garrity, L.J. Burgart, D.L. Riehle, E.M. Hill, T.J. Sebo, T. Witzig, Identifying and quantifying apoptosis: Navigating technical pitfalls, Mod. Pathol. 16 (2003) 389–394.
[83] B. Li, S. Zhang, N. Huang, H. Chen, P. Wang, J. Li, Y. Pu, J. Yang, Z. Li, Dynamics of the spleen and its significance in a murine H22 orthotopic hepatoma model, Exp. Biol. Med. 241 (2016) 863–872.
[84] D.I. Gabrilovich, S. Nagaraj, Myeloid-derived suppressor cells as regulators of the immune system, Nat. Rev. Immunol. 9 (2009) 162–174.
[85] M.D. Vesely, M.H. Kershaw, R.D. Schreiber, M.J. Smyth, Natural innate and adaptive immunity to cancer, Annu Rev. Immunol. 29 (2011) 235–271.
[86] V. Cortez-Retamozo, M. Etzrodt, A. Newton, P.J. Rauch, A. Chudnovskiy, C. Berger, R.J. Ryan, Y. Iwamoto, B. Marinelli, R. Gorbatov, R. Forghani, T. I. Novobrantseva, V. Koteliansky, J.L. Figueiredo, J.W. Chen, D.G. Anderson, M. Nahrendorf, F.K. Swirski, R. Weissleder, M.J. Pittet, Origins of tumor-

associated macrophages and neutrophils, Proc. Natl. Acad. Sci. USA 109 (2012) 2491–2496.
[87] E.C. Lee, M. Fitzgerald, B. Bannerman, J. Donelan, K. Bano, J. Terkelsen, D. P. Bradley, O. Subakan, M.D. Silva, R. Liu, M. Pickard, Z. Li, O. Tayber, P. Li, P. Hales, M. Carsillo, V.T. Neppalli, A.J. Berger, E. Kupperman, M. Manfredi, J. B. Bolen, B. Van Ness, S. Janz, Antitumor activity of the investigational proteasome inhibitor MLN9708 in mouse models of B-cell and plasma cell malignancies, Clin. Cancer Res. 17 (2011) 7313–7323.
[88] T. De Schutter, G. Andrei, D. Topalis, S. Duraffour, T. Mitera, L. Naesens, J. van den Oord, P. Matthys, R. Snoeck, Cidofovir treatment improves the pathology caused by the growth of human papillomavirus-positive cervical carcinoma xenografts in athymic nude mice, Cancer Lett. 329 (2013) 137–145.
[89] B. Mertens, T. Cristina de Araujo Nogueira, D. Topalis, R. Stranska, R. Snoeck, G. Andrei, Investigation of tumor-tumor interactions in a double human cervical carcinoma xenograft model in nude mice, Oncotarget 9 (2018) 21978–22000.
[90] R.K. Rampal, M. Pinzon-Ortiz, A.V.H. Somasundara, B. Durham, R. Koche, B. Spitzer, S. Mowla, A. Krishnan, B. Li, W. An, A. Derkach, S. Devlin, X. Rong, T. Longmire, S.E. Eisman, K. Cordner, J.T. Whitfield, G. Vanasse, Z.A. Cao, R. L. Levine, Therapeutic efficacy of combined JAK1/2, Pan-PIM, and CDK4/6 inhibition in myeloproliferative neoplasms, Clin. Cancer Res. 27 (2021) 3456–3468.
[91] L. Levy, I. Mishalian, R. Bayuch, L. Zolotarov, J. Michaeli, Z.G. Fridlender, Splenectomy inhibits non-small cell lung cancer growth by modulating anti-tumor adaptive and innate immune response, Oncoimmunology 4 (2015), e998469.
[92] J. Chun, S.M. Park, J.M. Yi, I.J. Ha, H.N. Kang, M.K. Jeong, Bojungikki-tang improves response to PD-L1 immunotherapy by regulating the tumor microenvironment in MC38 tumor-bearing mice, Front. Pharmacol. 13 (2022), 901563.
[93] K. Dorshkind, G.M. Keller, R.A. Phillips, R.G. Miller, G.C. Bosma, M. O'Toole, M. J. Bosma, Functional status of cells from lymphoid and myeloid tissues in mice with severe combined immunodeficiency disease, J. Immunol. 132 (1984) 1804–1808.
[94] S. Tanaka, Y. Saito, J. Kunisawa, Y. Kurashima, T. Wake, N. Suzuki, L.D. Shultz, H. Kiyono, F. Ishikawa, Development of mature and functional human myeloid subsets in hematopoietic stem cell-engrafted NOD/SCID/IL2rγKO mice, J. Immunol. 188 (2012) 6145–6155.
[95] F. Mollinedo, Neutrophil degranulation, plasticity, and cancer metastasis, Trends Immunol. 40 (2019) 228–242.
[96] M. Reis-Sobreiro, G. Roue, A. Moros, C. Gajate, J. de la Iglesia-Vicente, D. Colomer, F. Mollinedo, Lipid raft-mediated Akt signaling as a therapeutic target in mantle cell lymphoma, Blood Cancer J. 3 (2013), e118.
[97] M. Edagawa, J. Kawauchi, M. Hirata, H. Goshima, M. Inoue, T. Okamoto, A. Murakami, Y. Maehara, S. Kitajima, Role of activating transcription factor 3 (ATF3) in endoplasmic reticulum (ER) stress-induced sensitization of p53-deficient human colon cancer cells to tumor necrosis factor (TNF)-related apoptosis-inducing ligand (TRAIL)-mediated apoptosis through up-regulation of death receptor 5 (DR5) by zerumbone and celecoxib, J. Biol. Chem. 289 (2014) 21544–21561.
[98] H.C. Ku, C.F. Cheng, Master regulator activating transcription factor 3 (ATF3) in metabolic homeostasis and cancer, Front. Endocrinol. 11 (2020) 556.
[99] H. Wang, M. Jiang, H. Cui, M. Chen, R. Buttyan, S.W. Hayward, T. Hai, Z. Wang, C. Yan, The stress response mediator ATF3 represses androgen signaling by binding the androgen receptor, Mol. Cell Biol. 32 (2012) 3190–3202.
[100] T.S. Udayakumar, R. Stoyanova, M.M. Shareef, Z. Mu, S. Philip, K.L. Burnstein, A. Pollack, Edelfosine promotes apoptosis in androgen-deprived prostate tumors by increasing ATF3 and inhibiting androgen receptor activity, Mol. Cancer Ther. 15 (2016) 1353–1363.
[101] S.B. Kondapaka, S.S. Singh, G.P. Dasmahapatra, E.A. Sausville, K.K. Roy, Perifosine, a novel alkylphospholipid, inhibits protein kinase B activation, Mol. Cancer Ther. 2 (2003) 1093–1103.
[102] G.A. Ruiter, S.F. Zerp, H. Bartelink, W.J. Van Blitterswijk, M. Verheij, Anti-cancer alkyl-lysophospholipids inhibit the phosphatidylinositol 3-kinase-AKT/PKB survival pathway, Anticancer Drugs 14 (2003) 167–173.
[103] R.L. Vinall, K. Hwa, P. Ghosh, C.X. Pan, P.N. Lara Jr., R.W. de Vere, White, Combination treatment of prostate cancer cell lines with bioactive soy isoflavones and perifosine causes increased growth arrest and/or apoptosis, Clin. Cancer Res 13 (2007) 6204–6216.
[104] K.G. Chee, J. Longmate, D.I. Quinn, G. Chatta, J. Pinski, P. Twardowski, C.X. Pan, A. Cambio, C.P. Evans, D.R. Gandara, P.N. Lara Jr., The AKT inhibitor perifosine in biochemically recurrent prostate cancer: A phase II California/Pittsburgh cancer consortium trial, Clin. Genitourin. Cancer 5 (2007) 433–437.
[105] M. Wang, M.E. Law, R.K. Castellano, B.K. Law, The unfolded protein response as a target for anticancer therapeutics, Crit. Rev. Oncol. Hematol. 127 (2018) 66–79.
[106] S.C. Chiu, S.P. Chen, S.Y. Huang, M.J. Wang, S.Z. Lin, H.J. Harn, C.Y. Pang, Induction of apoptosis coupled to endoplasmic reticulum stress in human prostate cancer cells by *n*-butylidenephthalide, PLoS One 7 (2012), e33742.
[107] P.K.B. Nagesh, E. Hatami, P. Chowdhury, V.K. Kashyap, S. Khan, B.B. Hafeez, S. C. Chauhan, M. Jaggi, M.M. Yallapu, Tannic acid induces endoplasmic reticulum stress-mediated apoptosis in prostate cancer, Cancers 10 (2018) 68.
[108] J. Chang, S. Hu, W. Wang, Y. Li, W. Zhi, S. Lu, Q. Shi, Y. Wang, Y. Yang, Matrine inhibits prostate cancer via activation of the unfolded protein response/endoplasmic reticulum stress signaling and reversal of epithelial to mesenchymal transition, Mol. Med. Rep. 18 (2018) 945–957.
[109] Y. Zhang, F. Li, L. Liu, H. Jiang, H. Hu, X. Du, X. Ge, J. Cao, Y. Wang, Salinomycin triggers endoplasmic reticulum stress through ATP2A3 upregulation in PC-3 cells, BMC Cancer 19 (2019) 381.
[110] M.J. Kim, J.M. Ku, S.H. Hong, H.I. Kim, Y.Y. Kwon, J.S. Park, D.H. Jung, Y. C. Shin, S.G. Ko, *In vitro* anticancer effects of JI017 on two prostate cancer cell lines involve endoplasmic reticulum stress mediated by elevated levels of reactive oxygen species, Front. Pharmacol. 12 (2021), 683575.
[111] X. Li, D. Zhou, Y. Cai, X. Yu, X. Zheng, B. Chen, W. Li, H. Zeng, M. Hassan, Y. Zhao, W. Zhou, Endoplasmic reticulum stress inhibits AR expression via the PERK/eIF2α/ATF4 pathway in luminal androgen receptor triple-negative breast cancer and prostate cancer, NPJ Breast Cancer 8 (2022) 2.
[112] A. Estella-Hermoso de Mendoza, M.A. Campanero, H. Lana, J.A. Villa-Pulgarin, J. de la Iglesia-Vicente, F. Mollinedo, M.J. Blanco-Prieto, Complete inhibition of extranodal dissemination of lymphoma by edelfosine-loaded lipid nanoparticles, Nanomedicine 7 (2012) 679–690.
[113] A. Estella-Hermoso de Mendoza, M. Rayo, F. Mollinedo, M.J. Blanco-Prieto, Lipid nanoparticles for alkyl lysophospholipid edelfosine encapsulation: Development and *in vitro* characterization, Eur. J. Pharm. Biopharm. 68 (2008) 207–213.